



Synthesis and structural analysis of formamidinate-supported Mg complexes



Yi-Ju Tsai^a, Michael B. Pastor^a, Wenfeng Lo^b, Qinliang Zhao^{a,*}

^a Department of Chemistry, University of the Pacific, 3601 Pacific Avenue, Stockton, CA 95211, USA

^b Department of Chemistry, Yeshiva University, 2495 Amsterdam Avenue, New York, NY 10033, USA

ARTICLE INFO

Article history:

Received 11 April 2015

Received in revised form 6 May 2015

Accepted 7 May 2015

Available online 20 May 2015

Keywords:

Formamidinate

Synthesis

Magnesium complexes

Structural analysis

Conformation

ABSTRACT

Reactions of 2-mesitylmagnesium bromide with *N,N'*-diarylformamidines afforded five Mg compounds [(DPhF)Mg(THF)₂]₂(μ-Br)₂ (**1**), [D(3,5-Xyl)F]₂Mg(THF)₂ (**2**), [D(2,6-Xyl)F]₂Mg(THF) (**3**), [D(2-ⁱPrPh)F]MgBr(THF)₃ (**4**), and [D(2-^tBuPh)F]₂Mg(THF) (**5**). Complexes **1**, **2** and **4** displayed monomeric octahedral metal centers supported by formamidinates, bromide counter anions, and coordinating THF solvent molecules, while the metal cores in **3** and **5** were five-coordinated and in distorted square-pyramidal geometries. Detailed structural analysis indicated that only dimagnesium or mononuclear complexes were obtained through the use of formamidinate ligands. Ligands of increased steric demands resulted in the formation of monomeric complexes. Solvent molecules and counter anions that can coordinate to the metal cores further regulated the product conformation. Monoanionic formamidinates in the complexes, mostly featuring two nearly identical N–C bonds on the N–C–N backbone upon complexation, exhibited a symmetric bidentate chelating (η^2) coordination mode.

© 2015 Elsevier B.V. All rights reserved.

1. Introduction

Formamidinates [HC(NR)₂][−] (R = alkyl, aryl, or silyl), a subclass of amidinates ([R'C(NR)₂][−], R' = alkyl, aryl, amido or H) [1], have attracted considerable interest from inorganic chemists due to their convenient synthetic accessibility, vast tunability in terms of electronic and steric properties, and broad versatility in coordination modes [2]. Upon deprotonation of a formamidine, the negative charge on the formamidinate can delocalize across the N–C–N backbone, forming a four-electron-three-atom center (**I** in Scheme 1). The two equivalent N binding sites can bind a single metal atom [3] or two metal cores simultaneously as seen in the classical “lantern-type” bimetallic complexes [4]. The negative charge can also localize onto one N atom, resulting in an asymmetric backbone with an amide and an imine group (**II**) in which a portion or all of the three lone pairs of electrons can bind metal atoms [5].

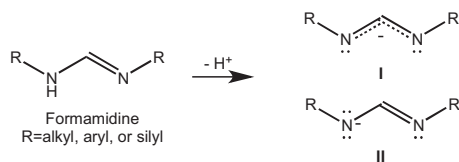
Another advantage of using formamidinates in coordination chemistry is the great tunability presented through derivatization. A large number of *N,N'*-diarylformamidine (DArFH) derivatives containing various substituents on the aryl rings (e.g. alkyl, alkoxy, halo and nitro groups) have been obtained and shown to support metal complexes [6]. The substituent modifications do not only

change the steric properties of the ligands but also their electronic properties, thus influencing the geometry and reactivities of the resulting metal complexes [7]. Modified formamidinate-supported metal complexes have established applications in catalyst development [8], material of photoelectronic properties [9] and atomic layer deposition [10].

There have been numerous amidinate-supported Mg complexes displaying a variety of conformations in the literature; [11] however, very few formamidinate-supported Mg complexes have been structurally characterized [12]. Overall, there are only four formamidinate-supported mononuclear Mg complexes Mg[D(*p*-Tol)F]₂(THF)₂ (**III** in Fig. 1, D(*p*-Tol)F = *N,N'*-di(*p*-tolyl)-formamidinate) [12a], Mg[D(*p*-Tol)F]₂(DME) (**IV**, DME = 1,2-dimethoxyethane) [12a], Mg[D(*p*-Tol)F]₂(TMEDA) (**V**, TMEDA = *N,N,N',N'*-tetramethylethylenediamine) [12a], Mg[D(*o*-Tol)F]₂(THF)₂ (**VI**, D(*o*-Tol)F = *N,N'*-di(*o*-tolyl)formamidinate) [12a], and two binuclear complexes [(DPhF)Mg(THF)]₂(μ-THF)(μ-Cl)₂ (**VII**, DPhF = *N,N'*-diphenylformamidinate) [12b], and {[D(2,6-ⁱPrPh)F]Mg(THF)}₂(μ-Cl)₂ (**VIII**, D(2,6-ⁱPrPh)F = *N,N'*-bis(2,6-diisopropylphenyl)formamidinate) [12c]. Comparison of synthesized Mg complexes supported by amidinates [11,12] and other ligands containing nitrogen coordinating sites [13] also revealed only monomeric or dimeric complexes with various metal–ligand ratios. Steric demands of the ligands played an important role in controlling the product geometry, whereas participation of other ions and molecules in coordination also has significant influence

* Corresponding author.

E-mail address: qzhao@pacific.edu (Q. Zhao).



Scheme 1. Lewis structures of formamidines.

over the product conformations. Here, we set to explore whether new conformations of magnesium complexes can be achieved by synthesizing and structurally characterizing complexes using formamidinate ligands of various steric demands, which were abbreviated as DPhFH, D(3,5-Xyl)FH, D(2,6-Xyl)FH, D(2-ⁱPrPh)FH and D(2-^tBuPh)FH (Fig. 2).

2. Results and discussion

2.1. Syntheses

All formamidine ligands were obtained by heating triethylorthoformate with 2-equiv. anilines without any solvent present, following literature methods [2]. Syntheses of the Mg complexes were accomplished by mixing the ligands with commercially available Grignard reagent 2-mesitylmagnesium bromide (MesMgBr) at $-35\text{ }^{\circ}\text{C}$. MesMgBr provided the Mg metal atoms and also acted as the internal base to deprotonate the formamidine ligands. Following Eq. (1), 2-equiv. DPhFH and 2-equiv. MesMgBr yielded bromide bridged bimetallic complex $[(\text{DPhF})\text{Mg}(\text{THF})_2]_2(\mu\text{-Br})_2$ (**1**). As described in Eqs. (2) and (3), reactions of 2-equiv. ligands of differing degrees of steric hindrance D(3,5-Xyl)FH, D(2,6-Xyl)FH or D(2-^tBuPh)FH and 2-equiv. MesMgBr in THF yielded bisformamidinate mononuclear complexes **2**, **3** and **5**, respectively, where only the number of coordinating THF molecules varies.

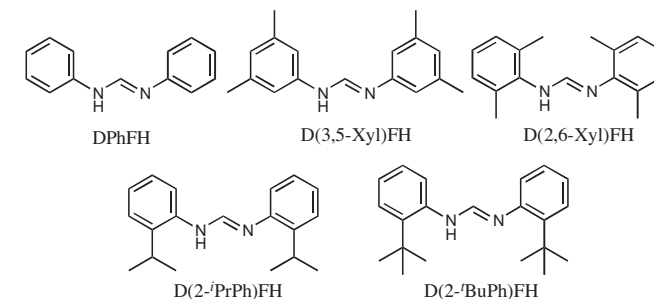


Fig. 2. Formamidines and their abbreviated names.

Complex **4** was obtained from D(2-ⁱPrPh)FH with 1 equiv. MesMgBr by following Eq. (4). Crystals of compounds **1–4** were obtained through evaporation diffusion at r.t. while complex **5** required a much lower temperature of $-35\text{ }^{\circ}\text{C}$ for successful crystallization, which may be due to the greater solubility of **5** in hexanes promoted by the $[\text{D}(2\text{-}^t\text{BuPh})\text{F}]^-$ ligands.

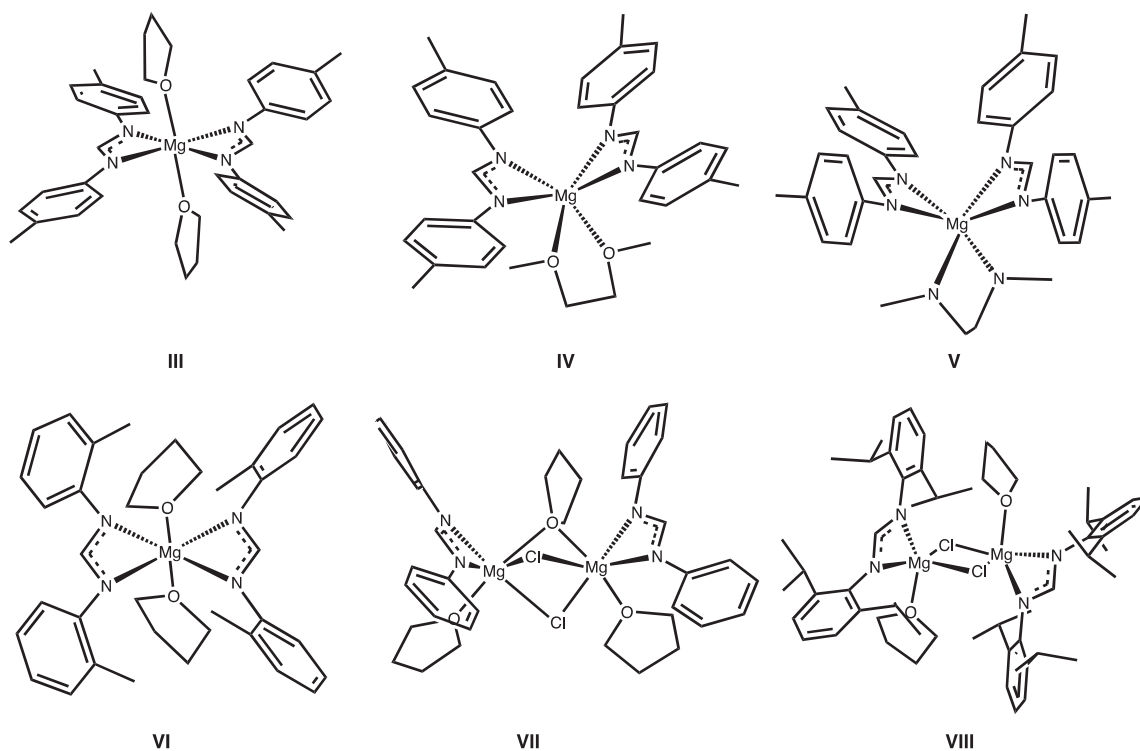
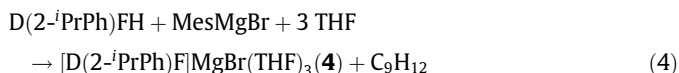
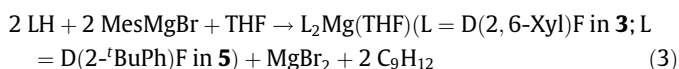
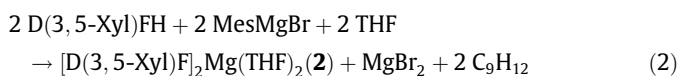
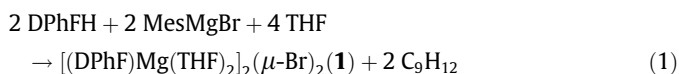


Fig. 1. Drawing of formamidinate-supported Mg complexes.

2.2. Structural analysis

Complex $[(\text{DPhF})\text{Mg}(\text{THF})_2]_2(\mu\text{-Br})_2$ (**1**) crystallized in the triclinic space group $P\bar{1}$ with two molecules containing nearly identical bond matrices in each unit cell. As shown in Fig. 3, each molecule was comprised of a dinuclear Mg_2Br_2 diamond core with two bromide bridges in the center. The center of the Mg_2Br_2 diamond core coincided with the inversion center of the molecule. The two Mg–N coordinative bonds with lengths of 2.154(1) and 2.140(1) Å were very short, which forced the Mg atom close to the C1 atom on the backbone (Mg1–C1: 2.526(2) Å, Table 1). Each Mg atom, in a *pseudo*-octahedral ligand environment, was supported by two monoanionic DPhF ligands in the equatorial plane and a THF molecule on either side of the plane. The separation between the two Mg centers was 3.651(1) Å with no net bonding between the metal atoms. The geometry of complex **1** resembled the geometry of **VIII** in Fig. 1, in which only one THF molecule was attached to each Mg center as a result of the high steric demand from the ligands [12c]. The core structure of **1** was also analogous to those possessed by the precursors that led to the discovery of the first two unusual Mg–Mg single bonds [14]. The C–N bond lengths on the N–C–N backbone of the formamidinate ligands were nearly identical, being 1.317(2) and 1.327(2) Å for C1–N1 and C1–N2, respectively. The symmetric feature of the N–C–N backbone demonstrated that the negative charge was delocalized, leading to a conjugated $\text{N}=\text{C}=\text{N}$ unit (**I**) with a symmetric bidentate chelating (η^2) coordination mode. Both formamidinates were equivalent in solid state as well as in solution, as a single set of signals was observed in NMR.

When D(3,5-Xyl)FH was applied as the ligand, a bisformamidinate mononuclear complex $[\text{D}(3,5\text{-Xyl})\text{F}]_2\text{Mg}(\text{THF})_2$ (**2** in Fig. 4), containing a nearly identical geometry to that of **III** and **VI** in Fig. 1, was obtained. Complex **2** crystallized in the monoclinic space group $C2/c$ with one half of the Mg molecule in an asymmetric unit. Mg1 resided on an inversion center that generated the other half of

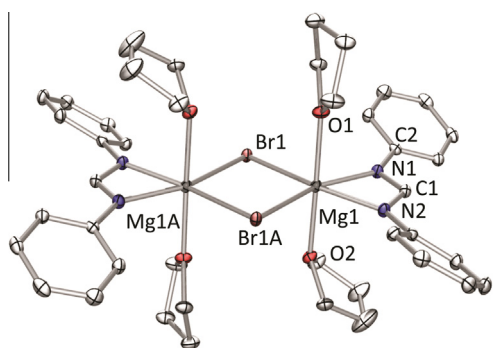


Fig. 3. X-ray crystal structure of **1**. Hydrogen atoms are omitted for clarity. Ellipsoids are shown at the 50% probability level.

Table 1

Selected non-bonded separations, bond lengths (Å) and angles (deg) in complex **1**.^a

Mg1...Mg1A	3.651(1)	C1–N1	1.317(2)
Mg1–N1	2.154(1)	C1–N2	1.327(2)
Mg1–C1	2.526(2)	N1–C2	1.406(2)
Mg1–N2	2.140(1)	N1–C1–N2	116.4(1)
Mg1–O1	2.144(1)	N1–Mg1–N2	63.11(5)
Mg1–O2	2.114(1)	C1–N1–Mg1	90.05(9)
Mg1–Br1	2.6355(7)	Mg1–Br1–Mg1A	87.29(2)
Mg1–Br1A	2.6547(6)	Br1–Mg1–Br1A	92.71(2)

^a Bond matrices of one molecule in a unit cell were shown. Those in the other molecule are nearly identical.

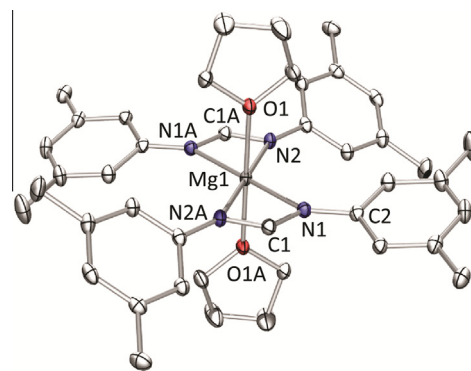


Fig. 4. X-ray crystal structure of **2**. Hydrogen atoms are omitted for clarity. Ellipsoids are shown at the 50% probability level.

Table 2

Selected bond lengths (Å) and angles (deg) in complexes **2** and **5**.

	2	5
Mg1–N1	2.1558(18)	2.1442(6)
Mg1–N2	2.1638(17)	2.1487(7)
Mg1–C1	2.532(2)	2.4642(8)
Mg1–O1	2.1154(15)	2.0318(9)
C1–N1	1.329(3)	1.3236(9)
C1–N2A	1.323(3)	1.3267(9)
N1–C2	1.395(3)	1.4204(9)
N1–C1–N2A	117.04(19)	118.15(7)
N1–Mg1–N2A	63.16(6)	63.96(2)
N1–Mg1–N2	116.84(6)	100.82(3)
N1–Mg1–N1A	180.0	144.52(4)
N2–Mg1–N2A	180.0	131.30(4)
N1–Mg1–O1	89.72(6)	107.74(2)
N1–Mg1–O1A	90.28(6)	
C1–N1–Mg1	89.97(13)	87.20(4)

the molecule. The coordination geometry about the magnesium center resembled a slightly distorted octahedron with two THF molecules in the axial positions. The Mg1 center and all four N atoms from the two D(3,5-Xyl)F anions were in the same equatorial plane and the linear O1–Mg1–O1A axis was completely perpendicular to the equatorial plane. Both D(3,5-Xyl)F anions were equivalent by symmetry in solid state as well as in solution as evidenced by a single set of signals observed in NMR. The two Mg–N bond lengths of 2.156(2) and 2.164(2) Å (Table 2) were similar to each other. The C–N bond lengths in the N–C–N backbone of the formamidinate ligands were 1.329(3) and 1.323(3) for C1–N1 and C1–N2A, respectively. Both formamidinate ligands in **2** exhibited the same bidentate chelating (η^2) coordination mode as those seen in **1**.

The bisformamidinate mononuclear complex $[\text{D}(2,6\text{-Xyl})\text{F}]_2\text{Mg}(\text{THF})$ (**3** in Fig. 5) contained a single magnesium center in a distorted square pyramidal geometry. Unlike **1** and **2**, only one additional THF molecule was bound to the Mg center in **3** due to the increased steric demand from the methyl groups on the *ortho*-positions of the aryl rings. The geometry of **3** resembled those of **IV** and **V** in which larger molecules DME and TMEDA (instead of THF) provided the extra support. Based on the bond matrices in Table 3, the complex contains a *pseudo*-C2 axis going through the Mg1–O1 bond. The Mg–N bond lengths varied significantly, with the short lengths of 2.083(5) and 2.082(5) Å and the longer lengths of 2.167(4) and 2.151(4) Å. All four C–N bonds in the N–C–N backbones of the formamidinate ligands were similar in length, with an average distance of 1.310[7] Å, indicating a bidentate chelating (η^2) coordination mode again for all formamidinates in **3**.

A mono-formamidinate complex $[\text{D}(2\text{-}^i\text{PrPh})\text{F}]\text{MgBr}(\text{THF})_3$ (**4** in Fig. 6) was attained through the installation of a single *iso*-propyl

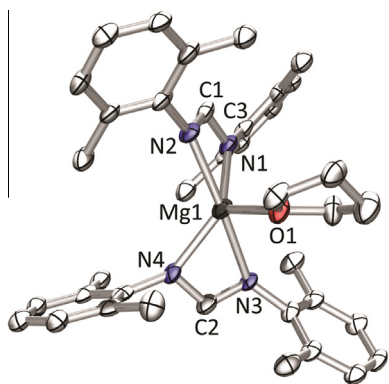


Fig. 5. X-ray crystal structure of **3**. Hydrogen atoms are omitted for clarity. Ellipsoids are shown at the 50% probability level.

Table 3
Selected bond lengths (Å) and angles (deg) in complex **3**.

Mg1–N1	2.083(5)	N1–C1–N2	117.2(5)
Mg1–N2	2.167(4)	N3–C2–N4	117.1(5)
Mg1–C1	2.483(6)	N1–Mg1–N2	63.62(17)
Mg1–N3	2.151(4)	N3–Mg1–N4	63.50(18)
Mg1–N4	2.082(5)	N1–Mg1–N3	113.99(19)
Mg1–C2	2.482(6)	N2–Mg1–N4	113.13(19)
Mg1–O1	2.050(4)	N1–Mg1–N4	131.3(2)
C1–N1	1.311(6)	N2–Mg1–N3	173.64(19)
C1–N2	1.315(6)	O1–Mg1–N1	115.95(18)
C2–N3	1.293(6)	O1–Mg1–N2	92.57(17)
C2–N4	1.319(6)	O1–Mg1–N3	93.74(17)
N1–C3	1.427(6)	O1–Mg1–N4	112.76(17)

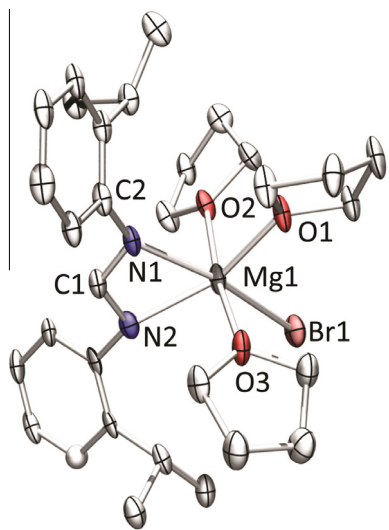


Fig. 6. X-ray crystal structure of **4**. Hydrogen atoms are omitted for clarity. Ellipsoids are shown at the 50% probability level.

group on the *ortho*-position of each phenyl ring. **4**, as a formamidinate-supported Mg complex, is unique in the sense that its geometry is different from any of those in the literature (Fig. 1) and from this study. The octahedral environment of the Mg center was composed of one formamidinate ligand, three THF molecules, and one bromide counter anion. Surprisingly, all three THF molecules were in the equatorial plane while the bromide was in the axial position, *trans* to one of the N atoms from the formamidinate. Selected bond lengths and angles are provided in Table 4. X-ray diffraction data for compound **4** was obtained at low quality, thus no detailed description of the bond lengths was provided here.

Table 4
Selected bond lengths (Å) and angles (deg) in complex **4**.^a

Mg1–N1	2.163(13)	N1–C1–N2	116.5(13)
Mg1–N2	2.230(12)	N1–Mg1–N2	61.5(4)
Mg1–C1	2.582(15)	N1–Mg1–O1	94.6(4)
C1–N1	1.343(18)	N1–Mg1–O2	94.0(4)
C1–N2	1.301(18)	N1–Mg1–O3	155.9(5)
N1–C2	1.425(18)	N1–Mg1–Br1	107.3(4)
Mg1–O1	2.130(11)	O1–Mg1–O2	170.8(5)
Mg1–O2	2.120(11)	O1–Mg1–Br1	87.9(3)
Mg1–O3	2.103(11)	O1–Mg1–O3	87.3(4)
Mg1–Br1	2.602(5)	Br1–Mg1–O3	96.7(3)
		O2–Mg1–O3	83.6(4)
		Br1–Mg1–O2	92.5(3)

^a Bond matrices of one molecule in an asymmetric unit were shown. Those in the other molecule are nearly identical.

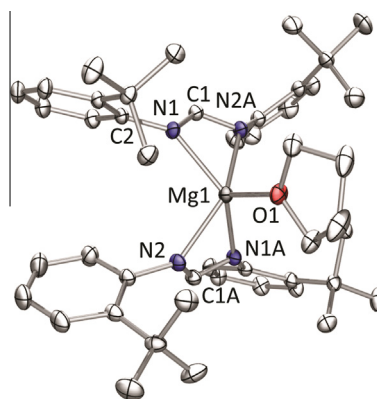


Fig. 7. X-ray crystal structure of **5**. Hydrogen atoms are omitted for clarity. Ellipsoids are shown at the 50% probability level.

Complex $[D(2\text{-}^t\text{BuPh})_2\text{Mg}(\text{THF})_2]$ (**5** in Fig. 7) crystallized in the monoclinic space group $C2/c$ with one half of the Mg molecule in an asymmetric unit. Atoms Mg1 and O1 from the THF molecule resided on a twofold axis that generated the other half of the molecule. Complex **5** also displayed a similar distorted square-pyramidal environment as seen in **3**. All four *tert*-butyl groups on the two formamidinates were directing toward the same side, leaving enough space for one single THF moiety. In comparison to **3**, the formamidinates in **5** bend further away from the Mg1–THF moiety due to the amplified steric demands from the *tert*-butyl groups. The two similar Mg–N bond lengths (2.1442(6) and 2.1487(7) Å, respectively) forced the Mg center close to the C1 atom with a short separation of 2.4642(8) Å (Table 2). Both formamidinates were related by symmetry, thus equivalent in solid state. The C–N bond lengths in the N–C–N backbone of the formamidinate ligands (1.3236(9) and 1.3267(9) Å for sC1–N1 and C1–N2A, respectively) indicated again a symmetric bidentate chelating (η^2) coordination mode for formamidinates in **5**.

Unlike Zn complexes of which clusters of various nuclearities have been demonstrated [15], only monomeric or dimeric Mg complexes supported by amidinates [11,12] and other nitrogen-containing ligands [13] were obtained. Steric properties of the ligands played an important role in dictating the product conformation and nuclearity. A halide-bridged dimagnesium complex (**1**) was observed when the simplest *N,N'*-diarylformamidinate was applied. Monomeric Mg complexes (**2**–**5**) were obtained when steric demands of the ligands were augmented by placing substituents on the aryl rings. This phenomenon bore a resemblance to that observed for amidinate-supported Mg complexes [11d]. Moreover, additional support for the Mg centers from the solvent molecules and counter anions further regulated the product conformation.

Table 5
Crystallographic data of Mg complexes 1–5.

	1 ^a	2 ^b	3 ^a	4 ^a	5 ^c
Chemical formula	C ₄₂ H ₅₄ Br ₂ Mg ₂ N ₄ O ₄	C ₄₂ H ₅₄ MgN ₄ O ₂	C ₃₈ H ₄₆ MgN ₄ O	C ₃₁ H ₄₇ BrMgN ₂ O ₃	C ₄₆ H ₆₂ MgN ₄ O
Formula weight	887.33	671.20	599.10	599.93	711.30
T (K)	100(2)	100(2)	100(2)	100(2)	150(2)
Space group	P $\bar{1}$	C2/c	P2 ₁ /n	P $\bar{1}$	C2/c
Z	2	4	4	4	4
a (Å)	9.3408(15)	11.2168(5)	12.431(5)	12.079(3)	14.2235(5)
b (Å)	9.8531(18)	19.2274(8)	14.968(5)	16.195(4)	15.9237(6)
c (Å)	23.049(4)	18.1729(9)	18.978(6)	16.500(4)	18.4845(7)
α (°)	88.356(8)	90	90	71.773(14)	90
β (°)	86.821(8)	105.0960(10)	108.43(2)	88.266(16)	99.420(2)
γ (°)	74.731(7)	90	90	89.095(16)	90
V (Å ³)	2043.1(6)	3784.1(3)	3350(2)	3064.4(13)	4130.1(3)
D _c (g cm ⁻³)	1.442	1.178	1.188	1.300	1.144
R ₁ (wR ₂) ^d (all data)	0.0311 (0.0703)	0.0980 (0.2320)	0.2224 (0.1944)	0.1844 (0.4266)	0.0628 (0.1574)
R ₁ (wR ₂) ^d [I > 2 σ (I)]	0.0234 (0.0593)	0.0745 (0.2021)	0.0835 (0.1532)	0.1474 (0.4092)	0.0495 (0.1444)
Goodness-of-fit (GOF)	1.104	1.187	1.039	1.104	1.079
CCDC deposition No.	1058607	1058608	1058609	1058610	1058611

^a Mo K α radiation.^b Monochromatic radiation ($\lambda = 0.44280$ Å).^c Monochromatic radiation ($\lambda = 0.7749$ Å).^d $R_1 = \sum ||F_o| - |F_c|| / \sum |F_o|$; $wR_2 = \{ \sum [w(F_o^2 - F_c^2)^2] / \sum [w(F_o^2)^2] \}^{1/2}$.

3. Conclusions

From the reactions between formamidine derivatives and MesMgBr, five new Mg compounds containing one halide-bridged dimeric and four mononuclear Mg complexes were obtained and structurally characterized. The Mg metal cores resided in either a *pseudo*-octahedral or a distorted square pyramidal environment. Structural analysis clearly demonstrated that the product geometry was strongly influenced by the size and position of the substituents on the ligands. Metallation of formamidinates with increased steric demands produced only monomeric complexes. Coordinating solvent molecules and counter anions were also involved in governing the product geometries. The monoanionic formamidinate ligands exhibited a symmetric bidentate chelating (η^2) coordination mode with the negative charge delocalized across the N–C–N backbone.

4. Experimental

4.1. General procedures

All manipulations were carried out using glove-box techniques under a nitrogen atmosphere. Glassware was oven-dried at 150 °C for a minimum of 10 h and cooled in an evacuated antechamber prior to use in the glove box. Hexanes and THF were dried and deoxygenated on a Glass Contour System (SG Water USA, Nashua, NH) and stored over 4 Å molecular sieves (Strem) prior to use. Chloroform-*d*₁ was purchased from Cambridge Isotope Labs, degassed and stored over 4 Å molecular sieves in the glove box prior to use. Non-halogenated solvents were typically tested with a standard purple solution of sodium benzophenone ketyl of THF in order to confirm effective oxygen and moisture removal. All *N,N'*-diarylformamidine ligands were prepared, following a procedure in the literature [2]. All other reagents were purchased from commercial vendors and used without further purification unless explicitly stated.

4.2. Synthesis of [(DPhF)Mg(THF)₂]₂(μ -Br)₂ (1)

4.803 g of a 1.0 M MesMgBr solution in THF (4.78 mmol), and 0.750 g DPhFH (3.82 mmol) were mixed in 15 mL of THF at –35 °C, giving a light yellow solution upon stirring. The mixture

was left stirring overnight at room temperature. Diffusion evaporation crystallization with hexanes slowly diffusing into the product solution of THF was set up at r.t. producing block-shaped clear crystals suitable for X-ray diffraction studies. The resulting crystals were collected by a frit, washed with hexanes (3 \times 1.0 mL) and then dried under vacuum. Crystal yield: 0.71 g, 41%. ¹H NMR (CDCl₃, 600 MHz, δ , ppm): 8.92 (s, 2H, N–CH–N), 7.26 (t, 8H, Ar–H), 7.21 (d, 8H, Ar–H), 6.92 (t, 4H, Ar–H), 4.05 (br, 16H, O–CH₂–CH₂ in THF), 1.86 (br, 16H, CH₂–CH₂–CH₂ in THF). ¹³C NMR (CDCl₃, 150 MHz, δ , ppm): 160.2, 149.1, 129.3, 121.0, 119.5, 69.94, 25.37. Anal. Calc. for C₄₂H₅₄Br₂Mg₂N₄O₄ (1): C, 56.85; H, 6.13; N, 6.31. Found: C, 56.68; H, 6.46; N, 6.29%.

4.3. Synthesis of [D(3, 5-Xyl)F]₂Mg(THF)₂ (2)

0.502 g of a 1.0 M MesMgBr solution in THF (0.50 mmol), and 0.200 g D(3,5-Xyl)FH (0.79 mmol) were mixed in 10 mL of THF at –35 °C, giving a light yellow solution upon stirring. The mixture was stirred overnight at room temperature. Diffusion evaporation crystallization was set up at r.t. using the THF solution with hexanes diffusing in, slowly producing block-shaped crystals suitable for X-ray diffraction studies. The resulting crystals were collected on a frit, washed with hexanes (3 \times 1.0 mL) and then dried under vacuum. Crystal yield: 0.054 g, 16% ¹H NMR (CDCl₃, 600 MHz, δ , ppm): 8.87 (s, 2H, N–CH–N), 6.78 (s, 8H, Ar–H), 6.58 (s, 4H, Ar–H), 4.00 (s, 8H, O–CH₂–CH₂ in THF), 2.26 (s, 24H, C–CH₃), 1.84 (s, 8H, CH₂–CH₂–CH₂ in THF). ¹³C NMR (CDCl₃, 150 MHz, δ , ppm): 161.0, 148.5, 138.6, 123.1, 117.5, 69.7, 25.30, 21.54.

4.4. Synthesis of [D(2,6-Xyl)F]₂Mg(THF) (3)

0.199 g of 1.0 M MesMgBr in THF (0.79 mmol) and 0.200 g D(2,6-Xyl)FH (0.40 mmol) were mixed in 10 mL of THF at –35 °C, giving a light yellow solution upon stirring. The mixture was stirred overnight at room temperature, and concentrated down to 1.0 mL under vacuum. The resulting light yellow milky solution with white precipitate was washed with hexanes (3 \times 1.0 mL) and then dried under vacuum to give 3 as a white powder. Isolated yield: 0.11 g, 92%. Diffusion evaporation crystallization was set up at r.t. using THF solution with hexanes diffusing in, slowly producing rectangular clear crystals suitable for X-ray diffraction studies. ¹H NMR (CDCl₃, 600 MHz, δ , ppm): 7.71, 7.00,

6.85 (14H, Ar-H and N-CH-N), 3.83 (br, 4H, O-CH₂-CH₂ in THF), 2.33 (br, 24H, Ar-CH₃) 1.79 (br, 4H, CH₂-CH₂-CH₂ in THF). ¹³C NMR (CDCl₃, 150 MHz, δ , ppm): 167.1, 133.0, 128.3, 125.3, 122.6, 69.83, 25.25, 19.94. Anal. Calc. for C₃₈H₄₆N₄OMg: C, 76.18; H, 7.74; N, 9.35. Found: C, 76.23; H, 7.78; N, 9.27%.

4.5. Synthesis of [D(2-ⁱPrPh)F]MgBr(THF)₃ (**4**)

2.258 g of 1.0 M MesMgBr solution in THF (2.25 mmol) and 0.500 g D(2-ⁱPrPh)FH (1.78 mmol) were mixed in 10 mL of THF at -35 °C, giving a light yellow solution upon stirring. The mixture was stirred overnight at room temperature, and then concentrated down to 1.0 mL under vacuum. The resulting light yellow milky solution with white precipitate was washed with hexanes (3 × 1.0 mL) and dried under vacuum to give **4** as a white powder. Isolated yield: 0.72 g, 67%. Diffusion evaporation crystallization was set up at r.t. using the THF solution with hexanes diffusing in, slowly producing clear block-shaped crystals suitable for X-ray diffraction studies. ¹H NMR (CDCl₃, 600 MHz, δ , ppm): 8.15 (s, ¹H, N-CH-N), 7.21–6.87 (m, 8H, Ar-H), 3.91 (br, 12H, O-CH₂-CH₂ in THF), 3.64 (sep, 2H, Ar-CH-(CH₃)₂), 1.84 (br, 12H, CH₂-CH₂-CH₂ in THF), 1.19 (d, 12H, -CH-(CH₃)₂). ¹³C NMR (CDCl₃, 150 MHz, δ , ppm): 166.0, 147.7, 141.7, 126.2, 125.5, 122.4, 121.3, 69.44, 27.26, 25.42, 23.53. Anal. Calc. for C₃₁H₄₇BrMgN₂O₃ (**4**): C, 62.06; H, 7.90; N, 4.67. Found: C, 61.86; H, 8.18; N, 4.68%.

4.6. Synthesis of [D(2-^tBuPh)F]₂Mg(THF) (**5**)

0.821 g of 1.0 M MesMgBr in THF (0.84 mmol) and 0.40 g D(2-^tBuPh)FH (1.30 mmol) were mixed in 10 mL of THF at -35 °C, giving a light yellow solution upon stirring. The mixture was stirred overnight at room temperature. Diffusion evaporation crystallization was set up using the THF solution with hexanes diffusing in at room temperature for 24 h and then at -35 °C, slowly producing clear block-shaped crystals suitable for X-ray diffraction studies. The resulting crystals were collected on a frit, washed with hexanes (3 × 1.0 mL) and then dried under vacuum. Crystal yield: 0.092 g, 20%. ¹H NMR (CDCl₃, 600 MHz, δ , ppm): 8.07 (s, 2H, N-CH-N), 7.28 (d, 4H, Ar-H), 7.06 (t, 4H, Ar-H), 7.00 (t, 4H, Ar-H), 6.63 (d, 4H, Ar-H), 3.91 (br, 4H, O-CH₂-CH₂ in THF), 1.84 (br, 4H, CH₂-CH₂-CH₂ in THF), 1.29 (s, 36H, -C-(CH₃)₃). ¹³C NMR (CDCl₃, 150 MHz, δ , ppm): 166.8, 148.0, 142.2, 126.5, 126.0, 125.6, 123.1, 70.2, 35.3, 25.2, 22.7.

5. X-ray structure determinations

Crystals were carefully sealed with Teflon- and Para-film in a capped vial and stored in a N₂ filled zip-lock bag before being shipped out for analysis. Single crystals suitable for X-ray analysis were coated with deoxygenated Paratone-N oil and mounted on Kapton loops. Crystallographic data for compounds **1**, **3**, and **4** were collected at 100(2) K on a Siemens (Bruker) SMART CCD area detector instrument with Mo K α radiation. Crystallographic data for compound **2** were collected on Beamline ChemMatCARS Sector 15 at the Advanced Photon Source, Argonne National Lab using monochromatic radiation ($\lambda = 0.44280$ Å) at 100(2) K. Crystallographic Data for compound **5** was collected on Beamline 11.3.1 at the Advanced Light Source, Lawrence Berkeley National Lab using monochromatic radiation ($\lambda = 0.7749$ Å) at 150(2) K. Raw data was integrated and corrected for Lorentz and polarization effects using Bruker APEX2 v. 2009.1 [16]. Absorption corrections were applied using SADABS [17]. Space group assignments were determined by examination of systematic absences, E-statistics, and successive refinement of the structures. The program PLATON [18] was employed to confirm the absence of higher symmetry for any of the crystals. The program CELL_NOW [19] was employed

to check and solve twinning problems of the crystals. The position of the heavy atoms was determined using direct methods in the program SHELXTL [20]. Subsequent cycles of least-squares refinement followed by difference Fourier syntheses revealed the positions of the remaining non-hydrogen atoms. Non-hydrogen atoms, excluding three carbon atoms in compound **4** were refined with anisotropic displacement parameters, and hydrogen atoms were added in idealized positions. Selected bond lengths, non-bonded separations, bond angles, and torsion angles are shown in Tables 1–4. Crystallographic data is shown in Table 5. Figures of X-ray crystal structures of complexes **1–5** (Figs. 3–7) were generated from Ortep-3 for Windows [21] and rendered using POV-Ray v3.6 for Windows [22].

6. Other physical measurements

Elemental analyses were performed by Complete Analysis Laboratories, Inc., Parsippany, New Jersey. ¹H and ¹³C NMR spectra were acquired on a JEOL ECA-600 NMR-spectrometer (600 MHz for ¹H and 150 MHz for ¹³C NMR) with spinning at r.t. Samples were sealed under a nitrogen environment before being sent for measurements.

Acknowledgments

We thank Dr. Vyacheslav V. Samoshin for the NMR measurements, Dr. Yu-Sheng Chen for his help with the single crystal measurement of compound **2**, and Dr. Simon J. Teat for his help with the single crystal measurement of compound **5**. We gratefully acknowledge the support from the Department of Chemistry at University of the Pacific, Pacific Fund and SAAG Grant at University of the Pacific, the NSF Major Research Instrumentation Grant (CHE-0722654) for the funding of JEOL ECA-600 NMR spectrometer, and the general user proposals for beam time at the Advanced Photon Source of Argonne National Laboratory and the Advanced Light Source of Lawrence Berkeley National Lab. ChemMatCARS Sector 15 is principally supported by the Divisions of Chemistry (CHE) and Materials Research (DMR), National Science Foundation, under grant number NSF/CHE-1346572. Use of the Advanced Photon Source, an Office of Science User Facility operated for the U.S. Department of Energy (DOE) Office of Science by Argonne National Laboratory, was supported by the U.S. DOE under Contract No. DE-AC02-06CH11357. The Advanced Light Source is supported by the Director, Office of Science, and Office of Basic Energy Sciences of the U.S. Department of Energy under Contract No. DE-AC02-05CH11231.

Appendix A. Supplementary material

CCDC 1058607 (**1**), 1058608 (**2**), 1058609 (**3**), 1058610 (**4**) and 1058611 (**5**) contains the supplementary crystallographic data for this paper. These data can be obtained free of charge from The Cambridge Crystallographic Data Centre via www.ccdc.cam.ac.uk/data_request/cif. Supplementary data associated with this article can be found, in the online version, at <http://dx.doi.org/10.1016/j.ica.2015.05.005>.

References

- [1] (a) F.T. Edelman, *Coord. Chem. Rev.* 137 (1994) 403; (b) J. Barker, M. Kilner, *Coord. Chem. Rev.* 133 (1994) 219; (c) D.A. KISSOUNKO, M.V. Zabalov, G.P. Brusova, D.A. Lemenovskii, *Russ. Chem. Rev.* 75 (2006) 351; (d) M.L. Cole, P.C. Junk, L.M. Louis, *J. Chem. Soc., Dalton Trans.* (2002) 3906; (e) M.L. Cole, D.J. Evans, P.C. Junk, M.K. Smith, *Chem. Eur. J.* 9 (2003) 415; (f) M.L. Cole, P.C. Junk, *J. Organomet. Chem.* 666 (2003) 55; (g) P.C. Junk, M.L. Cole, *Chem. Comm.* (2007) 1579.

- [2] (a) W. Marckwald, *Liebigs Ann. Chem.* 286 (1895) 343;
(b) E.C. Taylor, W.A. Ehrhart, *J. Org. Chem.* 28 (1963) 1108.
- [3] M.L. Cole, G.B. Deacon, C.M. Forsyth, K. Kristina, P.C. Junk, *Dalton Trans.* (2006) 3360.
- [4] F.A. Cotton, C.A. Murillo, R.A. Walton (Eds.), *Multiple Bonds Between Metal Atoms*, third ed., Springer Science and Business and Media Inc, New York, 2005.
- [5] (a) T.-G. Ong, G.P.A. Yap, D.S. Richeson, *Chem. Commun.* (2003) 2612;
(b) P.B. Hitchcock, M.F. Lappert, M. Layh, *J. Chem. Soc., Dalton Trans.* (1998) 3113;
(c) S. Bambirra, M.J.R. Brandsma, E.A.C. Brussee, A. Meetsma, B. Hessen, *J.H. Teuben, Organometallics* 19 (2000) 3197;
(d) Y.-C. Liu, W.-Y. Yeh, G.-H. Lee, S.-M. Peng, *Organometallics* 22 (2003) 4163.
- [6] (a) T. Ren, S. Radak, Y. Ni, G. Xu, C. Lin, K.L. Shaffer, V. DeSilva, *J. Chem. Crystallogr.* 32 (2002) 197;
(b) R. Anulewicz, I. Wawer, T.M. Krygowski, F. Männle, H.-H. Limbach, *J. Am. Chem. Soc.* 119 (1997) 12223;
(c) S.J. Archibald, N.W. Alcock, D.H. Busch, D.R. Whitcomb, *Inorg. Chem.* 38 (1999) 5571;
(d) T. Ren, C. Lin, P. Amalberti, D. Macikena, J.D. Protasiewicz, J.C. Baum, T.L. Gibson, *Inorg. Chem. Comm.* 1 (1998) 23;
(e) C.-W. Yeh, H.-L. Hu, R.-H. Liang, K.-M. Wang, T.-Y. Yen, J.-D. Chen, J.-C. Wang, *Polyhedron* 24 (2005) 539.
- [7] (a) T. Ren, *Coord. Chem. Rev.* 175 (1998) 43;
(b) K.M. Kadish, T.D. Phan, L. Giribabu, E.V. Caemelbecke, J.L. Bear, *Inorg. Chem.* 42 (2003) 8663.
- [8] N.V. Kulkarni, T. Elkin, B. Tumaniskii, M. Botoshansky, L.J.W. Shimon, M.S. Eisen, *Organometallics* 33 (2014) 3119.
- [9] A.A. Mohamed, H.E. Abdou, M.D. Irwin, J.M. Lopez-de-luzuriaga, J.P. Fackler Jr., *J. Cluster Sci.* 14 (2003) 253.
- [10] B. Lee, T.J. Park, A. Hande, K.J. Chung, M.J. Kim, R.M. Wallace, J. Kim, X. Liu, J. Yi, H. Li, M. Rousseau, D. Shenai, J. Suydam, *Microelectron. Eng.* 86 (2009) 1658.
- [11] (a) R.T. Boeré, M.L. Cole, P.C. Junk, *New J. Chem.* 29 (2005) 128;
(b) A. Xia, H.M. El-Kaderi, M.J. Heeg, C.H. Winter, *J. Organomet. Chem.* 682 (2003) 224;
(c) B.M. Day, W. Knowelden, M.P. Coles, *Dalton Trans.* 41 (2012) 10930;
(d) A.R. Sadique, M.J. Heeg, C.H. Winter, *Inorg. Chem.* 40 (2001) 6349;
(e) M.L. Cole, A.J. Davies, C. Jones, P.C. Junk, *New J. Chem.* 29 (2005) 1404;
(f) J.L. Sebestl, T.T. Nadasdi, M.J. Heeg, C.H. Winter, *Inorg. Chem.* 37 (1998) 1289;
(g) H.M. El-Kaderi, A. Xia, M.J. Heeg, C.H. Winter, *Organometallics* 23 (2004) 3488.
- [12] (a) M.L. Cole, D.J. Evans, P.C. Junk, L.M. Louis, *New J. Chem.* 26 (2002) 1015;
(b) F.A. Cotton, S.C. Haefner, J.H. Matonic, X. Wang, C.A. Murillo, *Polyhedron* 16 (1997) 541;
(c) P.C. Andrews, M. Brym, C. Jones, P.C. Junk, M. Kloth, *Inorg. Chim. Acta* 359 (2006) 355.
- [13] (a) W. Clegg, F.J. Craig, K.W. Henderson, A.R. Kennedy, R.E. Mulvey, P.A. O'Neil, D. Reed, *Inorg. Chem.* 36 (1997) 6238;
(b) M.G. Gardiner, G.R. Hanson, M.J. Henderson, F.C. Lee, C.L. Raston, *Inorg. Chem.* 33 (1994) 2456;
(c) J. Gao, Y. Liu, Y. Zhao, X.-J. Yang, Y. Sui, *Organometallics* 30 (2011) 6071;
(d) M. Gillett-Kunnath, W. Teng, W. Vargas, K. Ruhlandt-Senge, *Inorg. Chem.* 44 (2005) 4862;
(e) L. Bourget-Merle, M.F. Lappert, J.R. Severn, *Chem. Rev.* 102 (2002) 3031;
(f) W.E. Piers, D.J.H. Emslie, *Coord. Chem. Rev.* 233–234 (2002) 131;
(g) S. Westhusin, P. Gantzel, P.J. Walsh, *Inorg. Chem.* 37 (1998) 5956.
- [14] (a) S.P. Green, C. Jones, A. Stasch, *Science* 318 (2007) 1754;
(b) M. Westerhausen, *Angew. Chem., Int. Ed.* 47 (2008) 2185.
- [15] (a) M.B. Pastor, W. Lo, Q. Zhao, *Polyhedron* 97 (2015) 39;
(b) L.A. Lesikar, A.F. Richards, *Polyhedron* 29 (2010) 1411;
(c) C. Jones, L. Furness, S. Nembenna, R.P. Rose, S. Aldridge, A. Stasch, *Dalton Trans.* 39 (2010) 8788;
(d) F.A. Cotton, L.M. Daniels, L.R. Falvello, J.H. Matonic, C.A. Murillo, X. Wang, H. Zhou, *Inorg. Chim. Acta* 266 (1997) 91;
(e) M.L. Coles, D.J. Evans, P.C. Junk, L.M. Louis, *New J. Chem.* 26 (2002) 1015;
(f) N. Nimitsiriwat, V.C. Gibson, E.L. Marshall, P. Takolpuckdee, A.K. Tomov, A.J.P. White, D.J. Williams, M.R.J. Elsegood, S.H. Dale, *Inorg. Chem.* 46 (2007) 9988.
- [16] APEX2 v. 2009; Bruker Analytical X-Ray Systems Inc: Madison, WI, 2009.
- [17] G.M. Sheldrick, *SADABS*, Version 2.03; Bruker Analytical X-Ray Systems Inc: Madison, WI, 2000.
- [18] A.L. Spek, *PLATON*, A Multipurpose Crystallographic Tool, Utrecht University, Utrecht, The Netherlands, 2010.
- [19] G. M. Sheldrick, *CELL_NOW*. Version 2008/4. Georg-August-Universität Göttingen, Göttingen, Germany, 2008.
- [20] G.M. Sheldrick, *SHELXTL*, Version 6.14; Bruker Analytical X-Ray Systems Inc: Madison, WI, 2008.
- [21] L.J. Farrugia, *J. Appl. Crystallogr.* 45 (2012) 849.
- [22] Persistence of Vision Pty. Ltd.; Persistence of Vision (TM) Raytracer: Williamstown, Victoria, Australia, 2004.< <http://www.povray.org/>>.